

ChemComm

Chemical Communications

Accepted Manuscript

This article can be cited before page numbers have been issued, to do this please use: M. Huang, L. Yang, X. Li and G. Chang, *Chem. Commun.*, 2020, DOI: 10.1039/C9CC08699D.



This is an Accepted Manuscript, which has been through the Royal Society of Chemistry peer review process and has been accepted for publication.

Accepted Manuscripts are published online shortly after acceptance, before technical editing, formatting and proof reading. Using this free service, authors can make their results available to the community, in citable form, before we publish the edited article. We will replace this Accepted Manuscript with the edited and formatted Advance Article as soon as it is available.

You can find more information about Accepted Manuscripts in the [Information for Authors](#).

Please note that technical editing may introduce minor changes to the text and/or graphics, which may alter content. The journal's standard [Terms & Conditions](#) and the [Ethical guidelines](#) still apply. In no event shall the Royal Society of Chemistry be held responsible for any errors or omissions in this Accepted Manuscript or any consequences arising from the use of any information it contains.

COMMUNICATION

An indole-derived porous organic polymer for efficiently visual colorimetric capture of iodine in aqueous media via the synergistic effects of cation- π and electrostatic forcesReceived 00th January 20xx,
Accepted 00th January 20xx

DOI: 10.1039/x0xx00000x

Min Huang, Li Yang*, Xiuyun Li and Guanjun Chang*

We have successfully synthesized a new type of recyclable indole-based porous polymer, which possessed a high effective capture behavior for iodine in aqueous solution via the synergistic effects of cation- π and electrostatic forces. More interestingly, the absorption performance can be efficiently detected by a visual colorimetric assay through using a smartphone.

Nowadays, there is a large amount of radioactive waste caused by the development of the nuclear industry and medical diagnosis,^[1,2] which has created a serious threat to the livings within the ecosystem. Radioiodine (¹²⁹I and ¹³¹I), a typical radioactive pollutant, has already attracted public concerns as the volatile iodine can quickly spread into air and the environment resulting in radiological contamination would last over 10 million years, due to the 1.57 \times 10⁷ year radioactive half-life of ¹²⁹I.^[3] Indeed, radioiodine capable of eliciting a series of cytotoxic effects can cause serious health problems such as thyroid cancer.^[4] Thus, there is a challenging and fascinating task for the exploitation of readily accessible materials to effectively treat radioactive iodine waste.

Currently, a wide range of adsorbents have been designed and fabricated for iodine capture, including activated carbon,^[5] inorganic porous materials,^[6,7] metal-organic frameworks (MOFs)^[8] and porous organic polymers (POPs),^[9-16] etc. As one of the most promising candidates for the adsorption of iodine, POPs are an intriguing class of porous materials owing to their low densities, high surface areas, good thermal and chemical stabilities as well as tunable skeletons.^[10-12,17-18] Although POPs materials have been extensively investigated on the adsorption of iodine in volatile gas states or organic solvents,^[13,15-16] the construction of analytical methods for efficient detection and capture of iodine in water by POPs has

been less explored.^[19] Thus, designing new materials for operatively absorb iodine in aqueous solutions is important and necessary.

It is well-known that iodine uptake in a porous material is dependent on the pore environments, which means there should be existed active sites such as coordinative sites, Lewis acid-base sites, and electrostatic sites to interact with iodine.^[20] Nevertheless, these pores can be occupied by iodine at maximum accessibility of only 50% because of the coagulative and non-polar properties of iodine,^[21,22] which will inevitably lead to the poorer adsorption capacity. Recently, we described a series of indole-derived polymers with π -electronic-rich frameworks as outstanding adsorbents for electron-deficient analytes.^[23,24] Particularly, we have described a new concept for constructing of indole-based POPs as lithium-doped hydrogen adsorption materials via cation- π interactions.^[25] Enlightened by these studies mentioned above, we postulated a novel strategy for visual colorimetric extraction of iodine in aqueous media by using a smart phone via the synergistic effects of cation- π and electrostatic interactions within a new indole-based POP.

Herein, we performed the following concept. First, we established a new class of indole-derived POP (PTIBBL) via a facile Friedel-Crafts reaction (Fig. 1). Second, the obtained POP treated with sodium iodide would be particularly more attractive to absorb iodine, as the indole rings could be available for binding Na⁺ via the well-known cation- π interactions, and meanwhile, the Na⁺-indole complex could efficiently capture polyiodide anions^[26] through the electrostatic forces in aqueous solution. More interestingly, the yellow color of aqueous solution was fade when PTIBBL extracted iodine, allowing for visual detection. The present visual colorimetric assay is simple, portable and suitable for on-site detection in real water samples. This underlying design principle is illustrated schematically in Fig. 1.

The PTIBBL was rationally synthesized from a Friedel-Crafts alkylation reaction of 1,3,5-tris-(4-indolylbenzoyl)benzene (TIBB) with formaldehyde dimethylacetal (FDA). Detailed experimental procedures are provided in the ESI†. The as-obtained PTIBBL was a dark-yellow powder (Fig. 2) and the

State Key Laboratory of Environment-friendly Energy Materials, School of Material Science and Engineering, Southwest University of Science and Technology, Mianyang, 621010, P. R. China. E-mail: yanglichem628@126.com, gjchang@mail.ustc.edu.cn.

Electronic Supplementary Information (ESI) available: Details of the synthesis and characterization of PTIBBL; main materials and measurements; the analysis of I₂ absorption behaviour; visual colorimetric detection of iodine. See DOI: 10.1039/x0xx00000x

successful preparation of it was confirmed by Fourier-transform infrared (FT-IR), ^{13}C CP/MAS NMR as well as elemental analysis, and the results were in good agreement with the proposed structures (Scheme S3, Fig. S2 and Table S1). Thermogravimetric analysis (TGA) displayed an apparent weight loss began at temperature as high as 523 °C and still had high char yields at 800 °C, indicating the excellent thermal stability of PTIBBL (Fig. S3a). Furthermore, powder X-ray diffraction (XRD) of the sample was performed. PTIBBL showed a broad peak in the XRD pattern, suggesting that it was amorphous in nature (Fig. S3b).

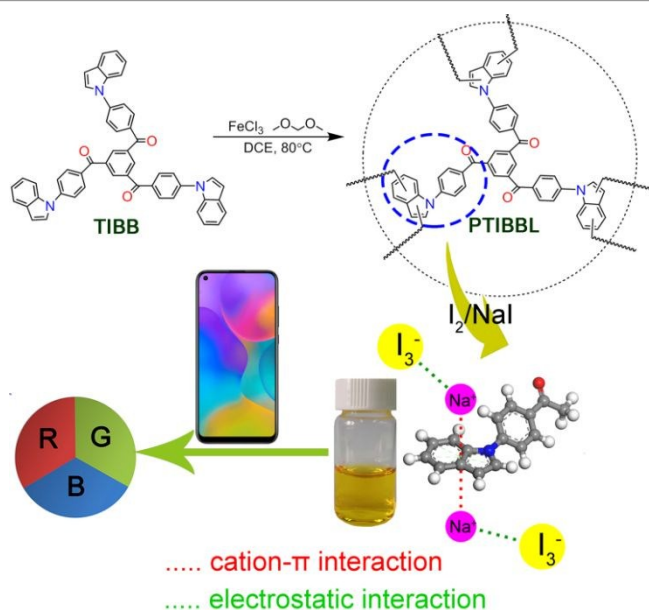


Fig. 1 Synthesis of PTIBBL and schematic illustration of the visual colorimetric capture of I_2 in aqueous solution via the synergistic effects of cation- π and electrostatic interactions.

We quantified the porosity of PTIBBL by scanning electron microscopy (SEM), transmission electron microscopy (TEM), and sorption analysis. The SEM image (Fig. 2a) exhibited that PTIBBL was consisted of aggregated particles with nonuniform pores. Moreover, a TEM image (Fig. 2b) revealed the porous structure, which is an essential requirement for iodine capture. At 77 K, the N_2 isotherms showed rapid uptake at a low pressure (0–0.1 bar), indicating a microporous nature (Fig. 2c). At a relatively high pressure (~ 0.9 bar), there was an increase in the N_2 sorption because of the interparticulate void associated with the meso- and macrostructures of the sample. The Brunauer-emmett-teller (BET) specific surface area of PTIBBL was calculated to be $399.1 \text{ m}^2 \cdot \text{g}^{-1}$. The pore size distribution of this polymer was calculated from the N_2 adsorption isotherms by the nonlocal density function theory (NLDFT) method, suggesting that PTIBBL possessed micropores centred at 1.23 nm and the pore volume was $0.367 \text{ cm}^3 \cdot \text{g}^{-1}$ (Fig. 2d).

As we know, I_2 could form I_3^- ion with binding I^- to improve its solubility in water^[27,28] and the color of solution would be altered to yellow. Thus, the kinetics was first studied to evaluate the adsorption rate of indole-based POP PTIBBL for I_2

in NaI aqueous solution. The adsorption amount increased rapidly in the initial 30 min, and then increased slowly to achieve equilibrium at about 6.5 h with an equilibrium adsorption capacity ($q_{e, \text{exp}}$) of 401.68 mg g^{-1} (Fig. S4a and Table S2). These results suggested that the adsorption rate of PTIBBL on iodine was very fast and these advantages would make PTIBBL be a potential material for iodine uptake. Furthermore, the correlation coefficient R^2 of the pseudo second-order kinetic model ($R^2 = 0.999$) was much higher than that of the pseudo-first-order kinetic model ($R^2 = 0.858$) for adsorption of I_2 (Fig. S4 and Table S2). And the calculated equilibrium adsorption capacity ($q_{e, \text{cal}}$) of 408.16 mg g^{-1} was reached. It was clear that the adsorption of I_2 on PTIBBL was a chemisorption process.

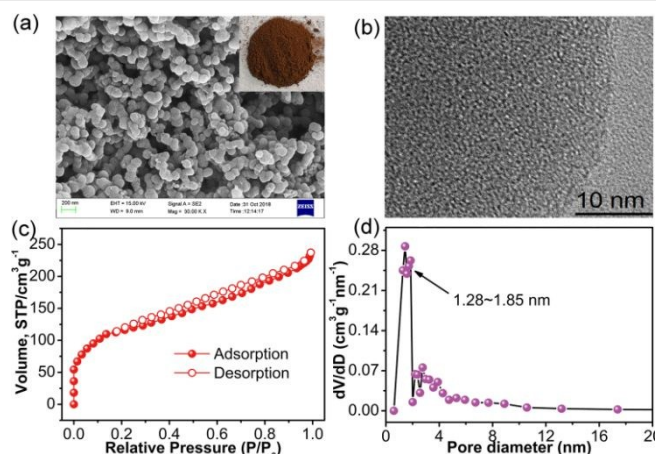


Fig. 2 (a) SEM image; inset: photograph of PTIBBL. (b) TEM image. (c) N_2 adsorption-desorption isotherm and (d) pore-size distribution of PTIBBL.

The fitting results of the adsorption isotherm models were displayed in Fig. S5. The Langmuir model ($R^2 = 0.999$) had a better correlation than the Freundlich model ($R^2 = 0.973$), demonstrating that the experimental adsorption process fitted well with the Langmuir equation. The results implied that the adsorption of I_2 was mainly monolayer adsorption and occurred on the surface of adsorbents. The maximum uptake capacity was 666.7 mg g^{-1} (Table S3). It was worth noting that the iodine loading capacity of PTIBBL was much higher than that of reported adsorbents shown in Table S4.^[13,15,21,28] More significantly, in order to assess the I_2 capture ability of PTIBBL, other ordinary porous materials such as activated carbon and molecular sieve were used for comparison. The same weights of different adsorbents (zeolite 13X, activated carbon and PTIBBL) were immersed in a solution of iodine (300 mg L^{-1}) at room temperature. Fig. S6 revealed the different extraction rates and capability of PTIBBL in comparison with zeolite 13X and activated carbon. The uptake of iodine on PTIBBL was very efficient, and obviously exceeded that of zeolite 13X and activated carbon in the aqueous media. It was inferred that the excellent affinity of PTIBBL for iodine resulted in the exceptional uptake of iodine compared to conventional iodine capture materials lacking an accessible interaction between the host and I_2 . As expect, these characteristics made PTIBBL a

promising and competitive candidate for radioactive iodine capture in aqueous media.

As displayed in Fig. 3a, the adsorption capacity of I_2 by PTIBBL increased as the initial concentration of I_2 increased and the color of the solution gradually changed from orange to light yellow or colorless after 48 hours (Fig. 3c), which suggested that iodine was encapsulated in indole-POP networks to continuously make iodine captured in solution. The removal efficiency of PTIBBL was calculated by the maximum uptake amount. In Fig. 3b, the highest removal efficiency reached as high up to 90.7%. With this uptake value, PTIBBL could be considered as outstanding absorbent for iodine solution than that of other porous materials (Table S4).^[13,15,21,28] By contrast, the uptake capacity of iodine for the polymer PTIBBL was much superior to that of the monomer TIBB (Fig. S7). This might be due to the richer porosity of PTIBBL for I_2 capture. To further confirm the form of iodine loaded in PTIBBL, the XPS spectrum was measured. It was turned out that the iodine existed as both neutral I_2 and I_3^- in PTIBBL^[19] (Fig. 3d). We considered that some adsorbed I_3^- ions were unstable in air and would be quickly transformed to I_2 molecules.^[26]

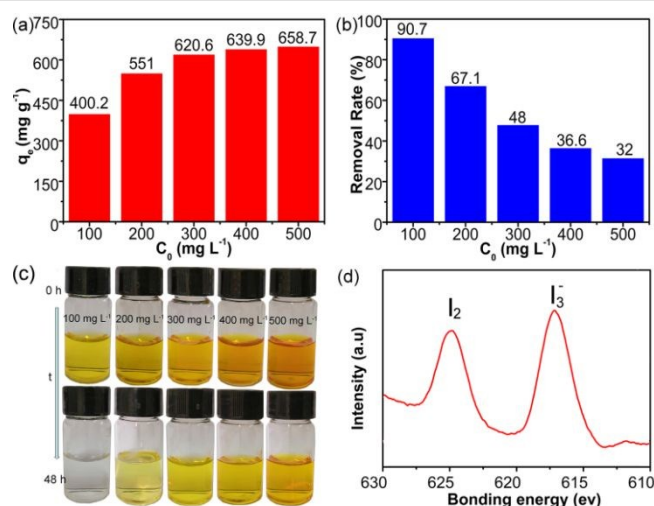


Fig. 3 (a) The adsorption of PTIBBL for iodine solution with different concentration from 100 to 500 mg L⁻¹. (b) The removal efficiency of PTIBBL for iodine solution. (c) Color change of iodine solution with different concentrations after adsorption for 48h. (d) XPS spectrum of iodine-loaded PTIBBL.

Subsequently, the iodine loaded on PTIBBL could be removed in ethanol. The reversibility of the extracting process was conducted for five times. We found that the samples that were subjected to multiple recycling treatments still showed nearly the same absorbing behavior as the original POP material (Fig. S8), suggesting that the indole-based POP could be reused and there were no secondary pollution problems. Meanwhile, the used material also had almost the same structure characterization as the original sample (Fig. S9-S10).

To shed light on the mechanism of interaction between PTIBBL and I_2 , the UV-vis titration of TIBB with I_2 in the NaI solution was carried out. Fig. 4a exhibited the absorption spectra of TIBB in the absence and presence of 3 equiv. Na⁺, together with the difference spectrum of TIBB-Na⁺ minus TIBB.

The spectrum distinctly disclosed a negative band at 228 nm and a weak positive band at 257 nm, ascribable to a Na⁺-TIBB cation- π interaction (Fig. 4a). The difference spectrum (dashed line) reflected a small red-shift of the strong B_b transition of the TIBB indole ring upon complexation with Na⁺.^[23,24,29] More importantly, upon addition with I_2 in the NaI solution, the λ_{max} of TIBB-Na⁺ continuously underwent a red shift to 291 nm along with a dramatic increase in absorbance, and a concomitant regular increase in absorbance at 354 nm was also observed (Fig. S11). This meant the formation of a complex between I_3^- and TIBB-Na⁺ in the ground state. To get more insight into the formation of complexes and the main binding interactions, the energy levels of the frontier orbitals were further calculated by using the DFT method. As can be seen from Fig. 4b and 4c, TIBB-Na⁺ structure unit showed a low unoccupied molecular orbital (LUMO) level of -3.61 eV, hinting its great electron affinities. The results indicated that I_3^- may transfer a portion of the charge to the electrically deficient indole-Na⁺ moiety and be more easily bound as they came to closer. In addition, due to the specific role of ketones in electron transport,^[30] we speculated that the carbonyl presumably promoted the capture of iodine on POP via the electrostatic forces.

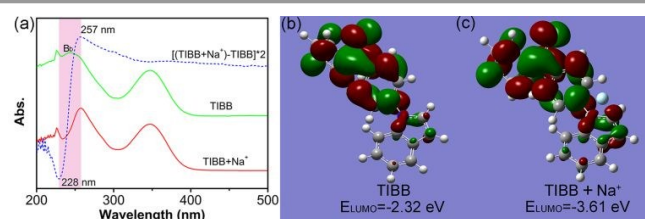


Fig. 4 (a) UV absorption spectra of TIBB (30 mM) and its 1:3 complex with NaI. The difference spectrum for TIBB-Na⁺ minus TIBB is doubly magnified for clarity. The interfacial plots of the LUMO orbital for TIBB structural unit (b) and TIBB-Na⁺ structural unit (c), respectively.

More gratifyingly, since the I_2 concentration directly correlated to the color of the aqueous solution, the corresponding optical images were collected by the camera of the smart phone and the RGB component change of the pictures was applied to quantitatively determine the iodine. Hence, the colorimetric response of the detection system toward iodine at different concentrations was investigated. Fig. 5a displayed the color tonality of the solution with various amounts of I_2 . As depicted in Fig. 5b, the standard curve was established as a linear relationship through the adjusted intensity and the logarithm of I_2 concentration in the range from 8 to 210 mg L⁻¹. The detection limit of this method was calculated to be 3.6 μ g L⁻¹ at a signal-to-noise ratio (S/N) of 3. This detection assay was comparable to or even better than that of previously reported methods for I_2 adsorption such as UV-vis spectra.^[13,28,31] Here, it is noted that the present method is cost-effective and does not involve any bulky equipment. Consequently, this assay is undoubtedly promising for on-site detection of radioiodine by using a portable smart phone.

Lastly, to evaluate the practical application of this colorimetric detection system, we applied it for I_2 capture in

natural water samples. Different concentrations of I_2 (50, 100 and 150 $mg\ L^{-1}$) were spiked to 100-fold diluted tap water and lake water with NaI, respectively, and analyzed by the present colorimetric method. As listed in Table 1, the removal rates ranged from 92.6% to 70.4% in the iodine lake wastewater. Besides, the I_2 -loaded wastewater samples were analyzed by this visual assay and UV spectra. The detection results from the presenting assay were well consistent with those tested by UV spectra (Table 2). All the results unambiguously attested that PTIBBL was qualified for practical application in efficient treatment of radioiodine pollutants by utilizing the present colorimetric assay.

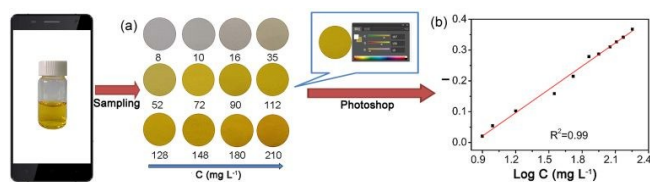


Fig. 5 Optical images of the detection aqueous solution after addition of different concentrations of I_2 in the range of 8-210 $mg\ L^{-1}$. (b) Linear relationship of the adjusted intensity (I) versus the logarithm of I_2 concentration from 8 to 210 $mg\ L^{-1}$.

Table 1 Adsorption results of iodine in natural water samples

Sample	C_0 ($mg\ L^{-1}$)	C_e ($mg\ L^{-1}$)	q_e ($mg\ g^{-1}$)	Removal rate (%)
Tap water	50	3.9	184.4	92.2
	100	9.7	361.2	90.3
	150	48.1	407.6	67.9
Lake water	50	3.7	185.1	92.6
	100	8.9	364.4	91.1
	150	44.5	422.2	70.4

Table 2 Comparison of detection results obtained in the analysis of iodine wastewater by this assay and UV spectra

Sample	I_2 capture by this assay ($mg\ L^{-1}$)	I_2 capture by UV spectra ($mg\ L^{-1}$)
1	2.91	3.15
2	15.34	15.47
3	43.50	43.87
4	49.99	50.24

In summary, we have rationally proposed a new type of recyclable indole-based porous polymer for effective extraction of iodine in aqueous media through the synergistic effects of cation- π and electrostatic interactions. More significantly, this capture behavior could be efficiently detected via a visual colorimetric assay by taking advantage of a smartphone. We anticipate that our strategy of developing this innovative adsorption system could be greatly extended to design and construct of advanced materials for the treatment of radioactive wastes or removing pollutants from aqueous environments.

This work was financially supported by the National Natural Science Foundation of China (No. 21973076, 21504073, 21202134, 11447215).

Conflicts of interest

There are no conflicts to declare.

Notes and references

View Article Online

DOI: 10.1039/C9CC08699D

- N. Yoshida and J. Kanda, *Science*, 2012, **336**, 1115-1116.
- P. C. Burns, R. C. Ewing and A. Navrotsky, *Science*, 2012, **335**, 1184-1188.
- L. VanMiddlesworth and J. Handl, *Health phys.*, 1997, **73**(4), 647-650.
- G. Mushkacheva, E. Rabinovich, V. Privalov, S. Povolotskaya, V. Shorokhova, S. Sokolova, V. Turdakova, E. Ryzhova, P. Hall, A. B. Schneider, D. L. Preston and E. Ron, *Radiat. Res.*, 2006, **166**, 715.
- R. Dawson, A. Laybourn, R. Clowes, Y. Z. Khimyak, D. J. Adams and A. I. Cooper, *Macromolecules*, 2009, **42**, 8809-8816.
- T. Hertzsch, F. Budde, E. Weber and J. Hulliger, *Angew. Chemie. Int. Ed.*, 2002, **41**, 2281-2284.
- H. Zou, F. Yi, M. Song, X. Wang, L. Bian, W. Li, N. Pan and X. Jiang, *J. Hazard. Mater.*, 2019, **365**, 81-87.
- D. Banerjee, X. Chen, S. S. Lobanov, A. M. Plonka, X. Chan, J. A. Daly, T. Kim, P. K. Thallapally and J. B. Parise, *ACS Appl. Mater. Interfaces*, 2018, **10**, 10622-10626.
- X. Guo, Y. Tian, M. Zhang, Y. Li, R. Wen, X. Li, X. Li, Y. Xue, L. Ma, C. Xia and S. Li, *Chem. Mater.*, 2018, **30**, 2299-2308.
- S. Das, P. Heasman, T. Ben and S. Qiu, *Chem. Rev.*, 2017, **117**, 1515-1563.
- Y. Xu, S. Jin, H. Xu, A. Nagai and D. Jiang, *Chem. Soc. Rev.*, 2013, **42**, 8012-8031.
- S. Das, P. Heasman, T. Ben and S. Qiu, *Chem. Rev.*, 2017, **117**, 1515.
- X. Qian, B. Wang, Z. Q. Zhu, H. X. Sun, F. Ren, P. Mu, C. Ma, W. D. Liang and A. Li, *J. Hazard. Mater.*, 2017, **338**, 224-232.
- Q. Sun, B. Aguila and S. Q. Ma, *Trends in Chemistry*, 2019, **1**, 292-303.
- S. Xiong, X. Tang, C. Pan, L. Li, J. Tang and G. Yu, *ACS Appl. Mat. Interfaces*, 2019, **11**, 27335-27342.
- X. He, S.-Y. Zhang, X. Tang, S. Xiong, C. Ai, D. Chen, J. Tang, C. Pan and G. Yu, *Chem. Eng. J.*, 2019, **371**, 314-318.
- K. Yuan, C. Liu, C. Liu, S. Zhang, G. Yu, L. Yang, F. Yang and X. Jian, *Polymer*, 2018, **151**, 65-74.
- K. Yuan, C. Liu, L. Zong, G. Yu, S. Cheng, J. Wang, Z. Weng and X. Jian, *ACS Appl. Mat. Interfaces*, 2017, **9**, 13201-13212.
- K. Jie, H. Chen, P. Zhang, W. Guo, M. Li, Z. Yang and S. Dai, *Chem. Commun.*, 2018, **54**, 12706-12709.
- P. Wang, Q. Xu, Z. Li, W. Jiang, Q. Jiang and D. Jiang, *Adv. Mater.*, 2018, 1801991.
- S. A. Y. Zhang, Z. Li, H. Xia, M. Xue, X. Liu and Y. Mu, *Chem. Commun.*, 2014, **50**, 8495-8498.
- H. Li, X. Ding and B. Han, *Chem. Eur. J.*, 2016, **22**, 11863-11868.
- G. Chang, Y. Wang, C. Wang, Y. Li, Y. Xu and L. Yang, *Chem. Commun.*, 2018, **54**, 9785-9788.
- P. Yang, L. Yang, Y. Wang, L. Song, J. Yang and G. Chang, *J. Mater. Chem. A*, 2019, **7**, 531-539.
- L. Yang, Y. Ma, Y. Xu and G. Chang, *Chem. Commun.*, 2019, **55**, 11227-11230.
- A. D. Awtrey, and R. E. Connick, *J. Am. Chem. Soc.*, 1951, **73**, 1842-1843.
- C. T. Hsieh and H. Teng, *Carbon*, 2000, **38**, 863-869.
- H. Sun, P. La, R. Yang, Z. Zhu, W. Liang, B. Yang, A. Li and W. Deng, *J. Hazard. Mater.*, 2017, **321**, 210-217.
- H. Yorita, K. Otomo, H. Hiramatsu, A. Toyama, T. Miura and H. Takeuchi, *J. Am. Chem. Soc.*, 2008, **130**, 15266-15267.
- E. Hayon, T. Iyata, N. N. Lichtin and M. Simic, *J. Phys. Chem.*, 1972, **76**, 2072-2078.
- B. Zheng, X. Liu, J. Hu, F. Wang, X. Hu, Y. Zhu, X. Lv, J. Du and D. Xiao, *J. Hazard. Mater.*, 2019, **368**, 81-89.

An indole-derived porous organic polymer for efficiently visual colorimetric capture of iodine in aqueous media via the synergistic effects of cation- π and electrostatic forces

Min Huang, Li Yang*, Xiuyun Li and Guanjun Chang*



Recyclable indole-based POP is successfully achieved, capable of visual colorimetric iodine capture in water via cation- π and electrostatic interactions.